CrossMark

ORIGINAL PAPER

Electrochemical synthesis, characterisation and comparative study of new conducting polymers from amino-substituted naphthalene sulfonic acids

Alemnew Geto [1,2] · Christopher M. A. Brett [2]

Abstract Conducting polymers have been synthesised electrochemically from 4-amino-3-hydroxynaphthalene-1-sulfonic acid (4A3HN1SA), 4-aminonaphthalene-1-sulfonic acid (4AN1SA) and 7-amino-4-hydroxynaphthalene-2-sulfonic acid (7A4HN2SA) on glassy carbon electrodes. The influence of the positive potential limit on the potential cycling polymerisation of 4A3HN1SA was studied, and a sufficiently high potential limit allowed better film growth. Under similar polymerisation conditions, the three monomers showed different radical formation potentials and different voltammetric peak profiles. The effects of scan rate and solution pH on the electrochemical properties of the polymers were investigated, in the range between 10 and 200 mV s^{-1}, all the modified electrodes showing a surface-confined electrode process. In the pH range from 2.0 to 9.0, the anodic peak potentials decreased linearly with increasing pH for all the three modified electrodes. The modified electrodes were characterised by electrochemical impedance spectroscopy in pH 4.0 and 7.0 buffer solutions. The results showed a more porous poly(7A4HN2SA) film, which is less affected by pH change than the other two films. Scanning electron microscopy of the polymer films also showed significant differences in their morphologies.

✉ Christopher M. A. Brett
cbrett@ci.uc.pt

1   Department of Chemistry, School of Natural and Computational Sciences, Samara University, Samara, Ethiopia

2   Department of Chemistry, Faculty of Sciences and Technology, University of Coimbra, 3004-535 Coimbra, Portugal

Introduction

Since their discovery, conducting polymers have attracted global attention in both research and industrial applications. The possibility of finding the combined properties of process-ability and flexibility of organic polymers and electronic properties of semiconductors and conductors in these materials is the main driving force for various applications [1]. Furthermore, their properties can be tailored electrochemically, mechanically, chemically and biochemically to suit specific applications, e.g. [2].

Among the conducting polymers, extensive work has been devoted to the study of only a few classes, such as polypyrrole, polyaniline, polythiophene and their derivatives [3]. However, recent trends show increasing interest in fused ring systems such as polynaphthalenes and their derivatives, owing to their remarkable inherent properties such as intense fluorescence, non-linear optical properties, strong π-stacking and good chemical stability. Such properties of naphthalene-based polymers and their derivatives allow the prospect of a considerable range of applications in various domains such as chemical sensors [4–11], batteries [12], electrochromic and electroluminescence devices [3, 13–16] and anti-corrosion coatings [17–21].

However, most of the reports to date have focused on co-polymers [6, 17, 21–23] or composites [7, 8, 12] which utilise naphthalenes or their substituted derivatives as one component. The use of naphthalenes and their derivatives in co-polymers and composites was found to impart uniformity

Springer

and stability to the polymer films [6], increase the selectivity [4] and catalytic activity [12] of chemical sensors, enhance corrosion protection efficiency [21], increase polymer processability [22] and surface reactivity [19].

Although some naphthalenes and their derivatives have been known for a long time to undergo homopolymerisation and co-polymerisation by both chemical and electrochemical routes, reports on their homopolymers are still limited. Hence, the synthesis and characterisation of homopolymers with high-quality and improved properties is needed and essential owing to their simplicity and potential use for new applications [17].

The polymerisation and applicability of 4-amino-3-hydroxynaphthalene-1-sulfonic acid has previously been demonstrated in the catalytic reduction of oxygen [12], anti-corrosion coatings [17, 20] and electrochemical determination of some biologically important compounds [8–10]. These reports showed excellent performance of the polymer film that served as a stable catalytic layer in modified electrodes and as an efficient corrosion inhibitor of different materials.

The monomer 4-amino-3-hydroxynaphthalene-1-sulfonic acid contains amino (–NH$_2$), hydroxyl (–OH) and sulfonic acid (–SO$_3$H) functional groups in its structure. The presence of such functional groups in monomers and their existence in the resulting polymer backbone plays an important role in various applications [22]. For instance, the existence of sulfonic acid groups in polymer chains helps to improve the solubility of the polymers in common polar solvents [19, 24]. Moreover, the polymers acquire an intrinsic proton doping ability leading to the formation of highly soluble self-doped homopolymers and co-polymers [22]. On the contrary, the extra benzene ring on substituted naphthalene molecules would confer greater hydrophobicity to the films formed from these materials (compared with their substituted benzene counterparts). It could also result in a lower degree of solvation, closer packing of the polymer chains, and reduced diffusion of solvated species through the film [4].

In addition, the presence of free –OH and –NH$_2$ in the polymer chain helps to promote attachment to other functional groups which can give the polymer film strong binding properties and good compatibility with other polymer layers and underlying surfaces [18].

In this work, the electrochemical potentiodynamic polymerisation of 4-amino-3-hydroxynaphthalene-1-sulfonic acid (4A3HN1SA) is investigated using different potential ranges and supporting electrolyte media. The optimum condition is then extended to polymerise and study the structurally similar monomers, 7-amino-4-hydroxynaphthalene-2-sulfonic acid (7A4HN2SA) and 4-aminonaphthalene-1-sulfonic acid (4AN1SA) (Fig. 1). After electrochemical polymerisation, the resulting polymer films from the three monomers were characterised by cyclic voltammetry, electrochemical impedance spectroscopy and scanning electron microscopy. To the
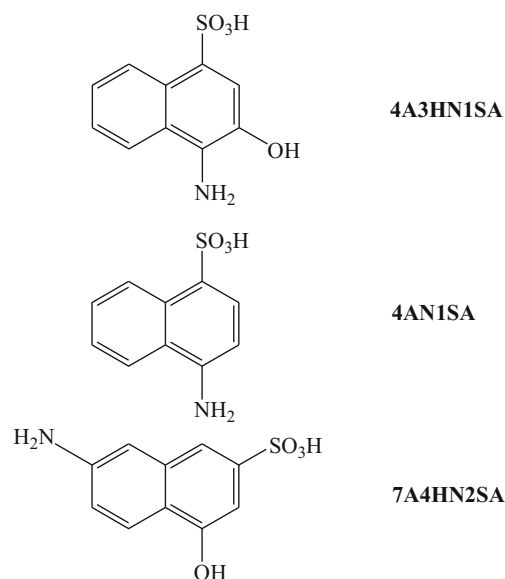

Fig. 1 Chemical structures of 4-amino-3-hydroxynaphthalene-1-sulfonic acid (4A3HN1SA), 4-aminonaphthalene-1-sulfonic acid (4AN1SA) and 7-amino-4-hydroxynaphthalene-2-sulfonic acid (7A4HN2SA)

best of our knowledge, the polymerisation and characterisation of 7-amino-4-hydroxynaphthalene-2-sulfonic acid and 4-aminonaphthalene-1-sulfonic acid has not been reported previously.

Experimental

Reagents and solutions

The monomers 4-amino-3-hydroxynaphthalene-1-sulfonic acid (4A3HN1SA), 4-aminonaphthalene-1-sulfonic acid (4AN1SA) and 7-amino-4-hydroxynaphthalene-2-sulfonic acid (7A4HN2SA) were purchased from Sigma-Aldrich. Britton-Robinson (B-R) buffer solutions were prepared from a mixture of boric acid (May and Baker Ltd.), acetic acid (Fischer Scientific Ltd.), 85 % phosphoric acid (Riedel-de Haen AG) and NaOH (Riedel-de Haen GmbH).

All chemicals were analytical reagent grade and used as received without prior purification. All aqueous solutions were prepared with Millipore Milli-Q nanopure water (resistivity ≥18 MΩ cm). All experiments were performed at room temperature (25 ± 1 °C).

Instrumentation

Electrochemical experiments were done using a potentiostat/galvanostat (Autolab PGSTAT30) connected to a computer with General Purpose Electrochemical System software (GPES v4.9) and frequency analysis software (FRA v4.9) from Metrohm-Autolab (Utrecht, Netherlands).

All experiments were carried out in a three-electrode cell using a modified or unmodified glassy carbon working electrode (3 mm diameter), a platinum wire as counter electrode and a silver/silver chloride (Ag/AgCl, 3 M KCl) as reference electrode. For impedance experiments, a sinusoidal voltage perturbation of 10 mV was applied, scanning from 65 kHz to 0.1 Hz, with ten measurement points per frequency decade. The equivalent circuit modelling was done with ZView3.2 software (Scribner Associates, Inc., USA). The pH measurements were done with a CRISON 2001 micropH-meter (Spain).

Scanning electron microscopy (SEM) was performed on films deposited on indium tin oxide (ITO) electrodes of area about 1 cm^2 with a Jeol JSM-5310 Scanning Microscope (JEOL, Inc., Peabody, MA, USA).

Electrode preparation

Prior to use, the glassy carbon electrode was polished with alumina powder and diamond spray of 1-µm diameter on a polishing cloth and thoroughly rinsed with ultrapure water (Milli-Q, Millipore).

The clean electrode was used to electropolymerise the respective monomer in a 0.1 M HNO$_3$ supporting electrolyte solution containing 2 mM 4A3HN1SA, 4AN1SA or 7A4HN2SA. Polymer film deposition was followed by a stabilisation step in a monomer free 0.5 M H$_2$SO$_4$ solution by scanning the potential between −0.8 and 0.8 V until a stable voltammogram was obtained.

For SEM measurements, polymer films were deposited on ITO electrodes by potential cycling for 60 cycles between −0.8 and 2.0 V (vs. Ag/AgCl) in 0.1 M HNO$_3$ solution containing 2 mM of the respective monomers. After coating, the electrodes were rinsed with water and allowed to dry under a nitrogen atmosphere.

Results and discussion

Electropolymerisation

The course of electropolymerisation by potential cycling can be influenced by several factors including potential scan rate, applied potential range, concentration of the monomer, type of supporting electrolyte, temperature and the electrode material [25, 26]. Preliminary studies were made on the effect of supporting electrolyte on the electropolymerisation of 4A3HN1SA in 0.1 M HNO$_3$ and 0.1 M H$_2$SO$_4$ solutions. The polymerisation was also carried out at different scan rates, and the results showed better polymerisation of 4A3HN1SA in 0.1 M HNO$_3$ at the scan rate of 100 mV s^{-1}.
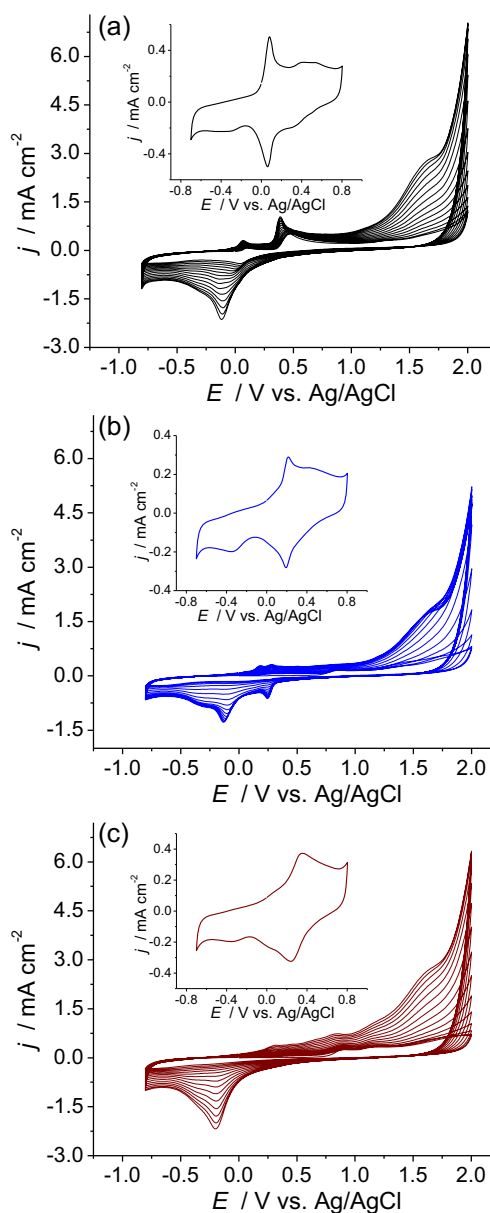

Fig. 2 Cyclic voltammograms obtained during the electropolymerisation of 2 mM **a** 4A3HN1SA, **b** 4AN1SA and **c** 7A4HN2SA in 0.1 M HNO$_3$ at a glassy carbon electrode between −0.8 and 2.0 V (vs. Ag/AgCl) for 15 cycles at 0.100 V s^{-1}. *Inset*: voltammograms recorded during film stabilisation in monomer-free 0.5 M H$_2$SO$_4$ between −0.8 and 0.8 V

Cyclic voltammograms showing electropolymerisation of the three monomers 4A3HN1SA, 4AN1SA and 7A4HN2SA in 0.1 M HNO$_3$ are given in Fig. 2.

The effect of positive potential limit on the polymerisation of 4A3HN1SA in 0.1 M HNO$_3$ at scan rate 100 mV s^{-1} was investigated by scanning the potential for 15 cycles from −0.8 to 1.6, 1.8 and 2.0 V (vs. Ag/AgCl). In the resulting voltammograms, higher current densities with faster growth of peaks were observed when the positive limit is set at 2.0 V followed by 1.8 and least with 1.6 V. The cyclic voltammograms recorded during polymerisation between −0.8 and 2.0 V, see

Fig. 2a revealed two additional peaks, one anodic at ca. 1.6 V and a sharp cathodic one at around −0.11 V. In [27], a similar reduction peak observed at −0.12 V (vs. Ag/AgCl) during the electropolymerisation of *p*-aminobenzene sulfonic acid in 0.1 M HNO_3 between −0.5 and 2.0 V was attributed to the inclusion of anions (NO_3^- and SO_4^{2-}) accompanied by hydrogenation of the polymer chain. However, in our work, scanning the potential in the same potential range using a clean electrode in monomer-free 0.1 M HNO_3 solution for 15 cycles gave a cathodic peak at −0.11 V and an anodic peak at 1.6 V but not the other peaks seen during polymerisation in the solution containing the monomer. These peaks at 1.6 and −0.11 V are therefore not related to the monomer or the resulting polymer film, but could correspond to electrode surface oxidation and reduction, respectively. A detailed discussion of the other peaks will be given below.

After each polymerisation, the electrodes were rinsed with water and transferred to monomer-free 0.5 M H_2SO_4 solution to stabilise the polymer film by removing unpolymerised adsorbed monomers and other loosely attached species. The applied potential was cycled until a stable voltammogram was obtained, indicating no additional adsorption or film degradation. The acid H_2SO_4 was chosen instead of HNO_3, since stable voltammograms were obtained after fewer potential cycles. This difference may be due to the higher conductivity of the sulphate ions present as well as to the lower pH.

Figure 3 shows voltammograms recorded in 0.5 M H_2SO_4 after 10 cycles of stabilisation of poly(4A3HN1SA) films, scanning between −0.8 and 0.8 V at 100 mV s^{-1}. Regardless of the potential window used to form the polymer, all electrodes had similar voltammetric profiles but different current densities, related to the amount of polymer film deposited on the electrode surface. The peak current recorded after polymerisation between −0.8 and 2.0 V is twofold and sixfold higher than that of films obtained after polymerisation at 1.8 and 1.6 V positive potential limits, respectively. Moreover, the maximum peak current and absence of any new peaks during stabilisation after polymerisation using a positive limit of 2.0 V shows the absence of film degradation during polymerisation. Therefore, it is necessary to apply a high positive potential to allow better growth of the 4A3HN1SA polymer film on the electrode surface. Hence, all further polymerisations were carried out between −0.8 and 2.0 V.

Figure 2a–c shows cyclic voltammograms obtained during the polymerisation of 4A3HN1SA, 4AN1SA and 7A4HN2SA, concentration 2 mM, respectively, in 0.1 M HNO_3 on a glassy carbon electrode between −0.8 and 2.0 V (vs. Ag/AgCl) for 15 cycles at 100 mV s^{-1}. Film stabilisation in monomer-free 0.5 M H_2SO_4 is shown in the insets. The anodic and cathodic peak potentials observed during the polymerisation process of the three monomers are summarised in Table 1. The presence of a broad anodic peak at high potentials and a sharp cathodic peak below −0.11 V is common to
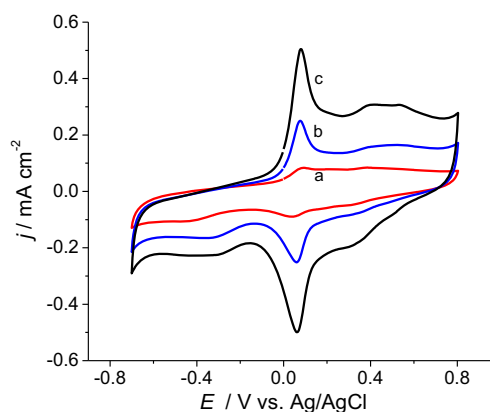

Fig. 3 Cyclic voltammograms during stabilisation of poly(4A3HN1SA)-modified glassy carbon electrode in 0.5 M H_2SO_4 after polymerisation between −0.8 V and **a** 1.6, **b** 1.8 and **c** 2.0 V

the three voltammograms, ascribed to surface oxidation and subsequent reduction in the presence of nitric acid, as discussed previously. All peaks are easily distinguishable on plotting individual cycles from the cyclic voltammograms in Fig. 2.

In the first cycle of 4A3HN1SA polymerisation, anodic peaks at potentials 0.10, 0.45 and 1.28 V and cathodic peaks at 0.26 and 0.05 V were observed. During 4AN1SA polymerisation, an anodic peak at 0.85 V, cathodic peaks at 0.25 and 0.05 V were seen in the first cycle. From the second cycle onwards, additional anodic peaks at 0.18 and 0.28 V started to appear and all peaks grew continuously with increasing cycle number. In the case of 7A4HN2SA, two anodic peaks at 0.91 and 1.18 V and two cathodic peaks at 0.23 and 0.0 V appeared during the first potential cycle. Repetitive potential scanning resulted in an additional broad anodic peak around 0.50 V and the increase in the height of all the peaks, showing the growth of polymer film at the electrode surface. Unlike 4ANSA, 4A3HN1SA and 7A4HN2SA have –OH in their structure. The additional oxidation peak seen in the first cycle of polymerization in the latter two is probably due to the oxidation of the hydroxyl group, as in [28]. To confirm the actual groups involved in the process, additional investigations are needed.

Comparing the cyclic voltammograms during the formation of the three polymers, as well as those of the stabilised polymer films, there are clear differences in peak profiles and

Table 1 Anodic, E_{pa}, and cathodic, E_{pc}, peak potentials vs. Ag/AgCl observed during the polymerisation of 4A3HN1SA, 4AN1SA and 7A4HN2SA in 0.1 M HNO_3 containing 2 mM monomer

Monomer	E_{pa}/V			E_{pc}/V	
4A3HN1SA	0.10	0.45	1.28	0.26	0.05
4AN1SA	0.18[a]	0.28[a]	0.85	0.25	0.05
7A4HN2SA	0.50[a]	0.91	1.18	0.23	0.00

[a] Peaks observed starting in the second cycle

peak positions, reflecting structural differences of the electroactive moieties of the monomers and the resulting polymers. Polymerisation of such monomers can be expected to occur through the $-NH_2$ groups, as suggested in [22], with the other aromatic ring in the case of in the case of 4A3HN1SA and 4AN1SA and the same aromatic ring (owing to steric effects) for 7A4HN2SA. The anodic peaks observed at 1.28, 0.85 and 1.18 V during the electropolymerisation, respectively, of 4A3HN1SA, 4AN1SA and 7A4HN2SA can be attributed to oxidation of the monomers, at the positively charged amine group $-NH_3^+$, in the acidic medium, leading to radical formation. The other peaks appearing after the first cycle (see Table 1) could correspond to the oxidation and reduction of intermediate species and the resulting polymers. Comparing the values for 4A3HN1SA and 4AN1SA, both $-NH_3^+$ and $-SO_3H$ have a negative inductive effect, this being reduced by the addition of the $-OH$ group, which stabilises the monomer so that 4A3HN1SA (with $-OH$ in position 3) is oxidised at a higher potential than 4AN1SA (without $-OH$). The monomer 7A4HN2SA is less directly affected by the $-SO_3H$ and $-OH$ groups in the other aromatic ring, although electron delocalisation can be expected to stabilise the charged monomeric species, the result being a value intermediate between 4A3HN1SA and 4AN1SA.

Characterisation of the polymer films

Cyclic voltammetry

The electrochemical behaviour of the polymer film modified electrodes was studied in 0.5 M H_2SO_4 solution at scan rates between 10 and 200 mV s^{-1} in the potential range between −0.8 and +0.8 V. For all three polymer-modified electrodes, both anodic and cathodic peak currents increased linearly with increasing scan rate over the range investigated. The values of the slopes of anodic and cathodic peak current densities (j_{pa} and j_{pc}) vs. scan rate (ν) plots for poly(4A3HN1SA)-, poly(4AN1SA)- and poly(7A4HN2SA)-modified glassy carbon electrodes are shown in Table 2. The results imply surface-controlled electron transfer processes of the polymer coatings [29].

The effect of solution pH on the electrochemical behaviour of the polymer film modified electrodes was also investigated in Britton-Robinson (B-R) buffer solutions of pH 2.0–9.0. The voltammograms obtained in solutions of different pH at the three polymer-modified electrodes are shown in Fig. 4.

For all the polymer-modified electrodes, the anodic and cathodic peaks gradually shifted towards less positive potentials as the pH increased from 2.0 to 9.0. The anodic peak potential shift with solution pH as observed from the plots were −69 mV pH^{-1} for both poly(4A3HN1SA) and poly(7A4HN2SA) and −60 mV pH^{-1} in poly(4AN1SA)-modified electrodes. These values are close to the theoretical value

Table 2 Slopes of the anodic and cathodic peak current densities (j_{pa} and j_{pc}) vs. scan rate calculated from cyclic voltammograms recorded in 0.5 M H_2SO_4 solution at scan rates from 10 to 200 mV s^{-1}

Polymer	j_{pa} (mA cm^{-2}/mV s^{-1})	j_{pc} (mA cm^{-2}/mV s^{-1})
poly(4A3HN1SA)	0.130	−0.149
poly(4AN1SA)	0.116	−0.104
poly(7A4HN2SA)	0.178	−0.142

for a redox process involving an equal number of protons and electrons.
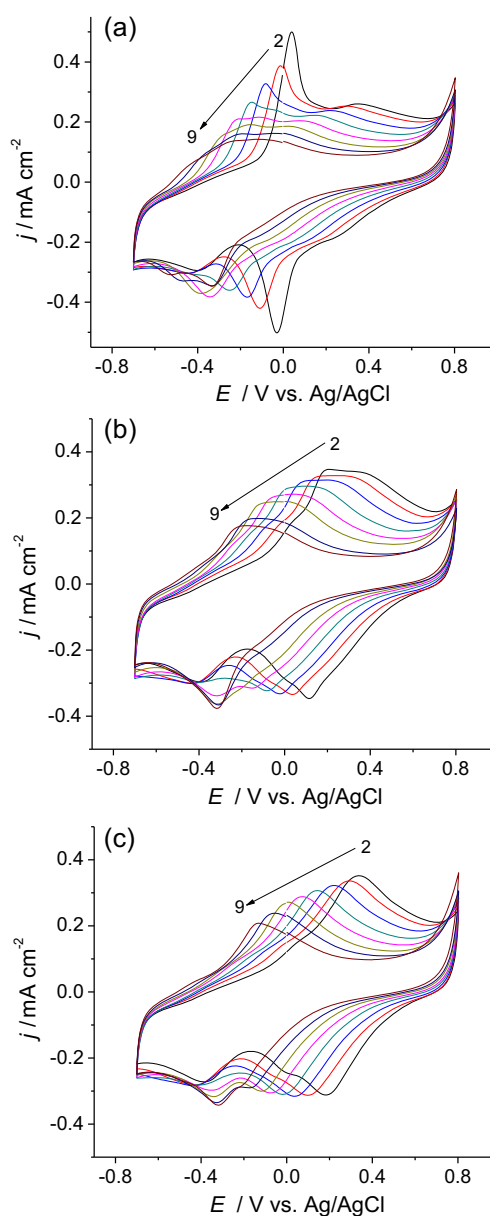

Fig. 4 Cyclic voltammograms obtained in B-R solutions between pH 2.0 and 9.0 at **a** poly(4A3HN1SA)/GCE, **b** poly(4AN1SA)/GCE and **c** poly(7A4HN2SA)/GCE after polymerisation between −0.8 and 2.0 V

The increase in solution pH resulted in a decrease in the anodic and cathodic peak currents in all the three modified electrodes. Comparing the anodic peaks obtained at pH 2.0 and 9.0, the decrease in peak current is significant in poly(4A3HN1SA) (84 %) followed by poly(4AN1SA) (50 %) and least in poly(7A4HN2SA) (41 %) modified electrode. This could be due to a slow decrease in the electrochemical activity of the polymer films and/or degradation of the films from the electrode surface with increasing pH. Repeating the sequence of experiments (from pH 2 to pH 9) showed that the effect of the increase in pH is partly reversible, corroborating this explanation. For example, at pH 4, the anodic peak current in the second series of measurements is less by 35 % for poly(4A3HN1SA), 15 % for poly(4ANSA) and 10 % for poly(7A4HN2SA), this decrease doubling after having reached pH 9. Thus, for future applications, care must be taken in using the modified electrodes in high pH media, particularly at more positive potentials.

Previously, the solubility of aniline-aminonaphthalene sulfonic acid co-polymer with different ratios of aniline to aminonaphthalene sulfonic acid had been investigated in 0.2 M NaOH solution. The decrease in the molar ratio of aniline to aminonaphthalene sulfonic acid resulted in an increase in the solubility of the co-polymer because of the greater number of $-SO_3H$ groups in the polymer backbone, which can become a water-soluble salt in alkaline medium [30].

Despite the presence of some similar functional groups in the monomers used, the difference in the rate of current change with increasing pH in the polymers can be partly attributed to the difference in the solubility of the films in high pH solutions, tested up to pH 9. This in turn could be related to the different relative positions of the functional groups in the polymer backbone. In addition, the better stability of poly(7A4HN2SA) at higher pH compared to the others makes it a promising candidate for electrochemical sensors and other potential applications that require stable films over a broader pH window.

Electrochemical impedance spectroscopy

Electrochemical impedance spectroscopy (EIS) was used to characterise the physical and interfacial properties of the polymer-modified electrodes; complex plane impedance spectra are shown in Fig. 5. Impedance spectra in 0.5 M H_2SO_4 at 0.045 V (vs. Ag/AgCl) of poly(4A3HN1SA)-modified glassy carbon electrodes, prepared by polymerisation at different positive potential limits are shown in Fig. 5a. Spectra for the three types of polymer-modified electrodes in B-R buffer solutions of pH 4.0 and 7.0 at different applied potentials are given in Fig. 5b–d.

Figure 6 shows the three equivalent electrical circuits that gave the best fits to the experimental spectra. The circuit elements used in different combinations were cell resistance (R_Ω), charge transfer resistance (R_{ct}), constant phase element (CPE) and the Warburg element (Z_W). The R_Ω is composed of the solution and the bulk composite resistances, and R_{ct} represents the charge transfer at the solid-liquid interface. The CPE represents the interfacial or polymer film charge separation, modelled as a non-ideal capacitor (CPE = $[(Ci\omega)^\alpha]^{-1}$), where $0.5 < \alpha < 1$, when $\alpha = 1$, the CPE corresponds to a pure capacitor. The Warburg impedance Z_W is modelled as an open circuit finite linear diffusion element defined by $Z_W = R_W coth[(\tau i\omega)^\alpha](\tau i\omega)^{-\alpha}$, where R_W is the diffusion resistance of electroactive species, τ is the diffusion time constant and $\alpha = 0.5$ for a perfectly uniform flat interface.
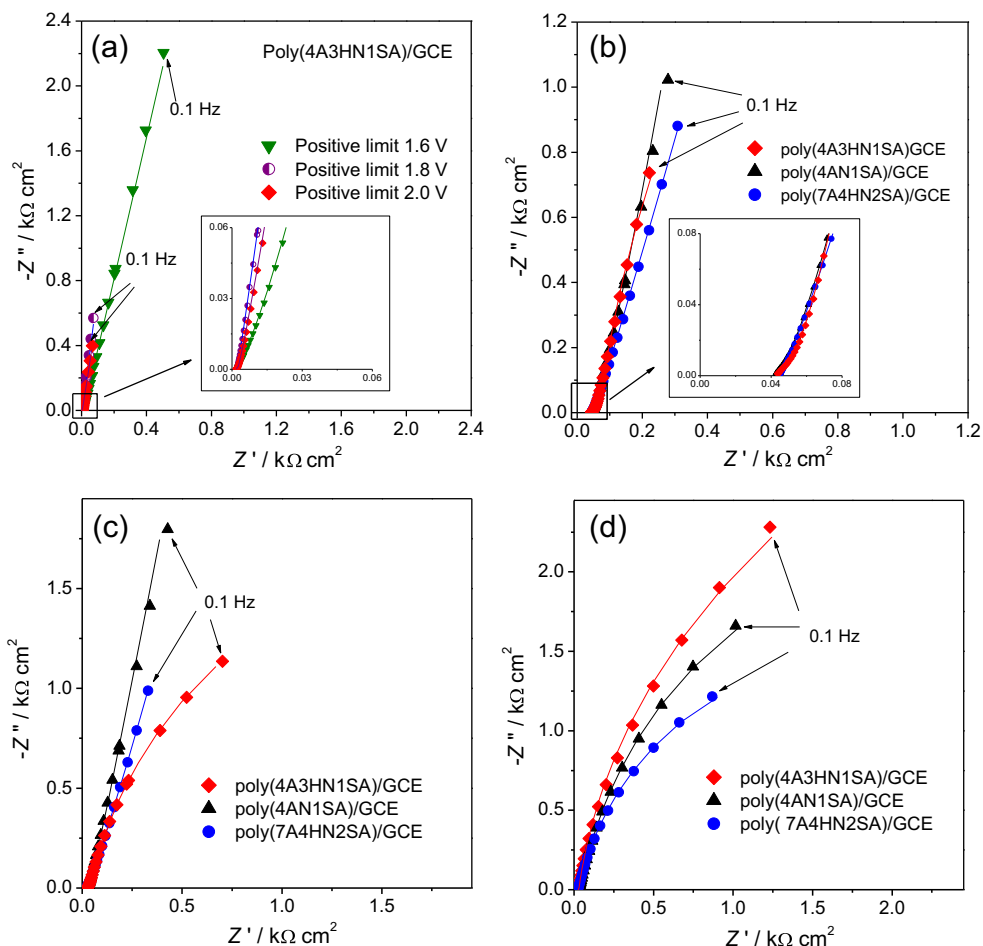
Figure 5a shows impedance spectra at poly(4A3HN1SA)-modified glassy carbon electrodes, prepared by electropolymerisation at different positive potential limits, in 0.5 M H_2SO_4 at an applied potential of 0.045 V (vs. Ag/AgCl)), close to the midpoint between the anodic and cathodic potentials of the major peaks in the cyclic voltammogram obtained using the modified electrode. Two equivalent circuits are proposed to fit the EIS results. When the positive limit is set at 1.6 V, the equivalent electrical circuit consists of R_Ω in series with a parallel combination of CPE_1 and R_{ct}, in series with CPE_2, the latter representing the bulk redox capacitance of the film that has been formed (Fig. 6a). The equivalent electrical circuit of Fig. 6b is used for fitting both the 1.8 and 2.0 V positive limit polymerised films which consists of R_Ω in series with CPE representing charge separation at the polymer-solution interface in series with Z_W representing diffusion in the film. The values of circuit elements calculated by fitting the spectra are summarised in Table 3.

The polymer-modified electrode prepared by polymerisation at 1.6 V positive potential limit has a significantly higher impedance magnitude of ~2.2 kΩ cm^2 at 0.1 Hz than those obtained at 1.8 V of ~0.6 kΩ cm^2 and 2.0 V of ~0.4 kΩ cm^2 (see Fig. 5a). This is in agreement with cyclic voltammetry (Electropolymerisation section), where the maximum peak current is obtained after polymerisation at the 2.0 V positive limit and the least at 1.6 V.

The higher impedance value and the need for a different equivalent circuit for the 1.6 V limit is a reflection of the change in both resistivity and electrode surface structure with the change in the positive potential limit during polymer film formation. An application of a lower switching potential may lead to inadequate polymer formation, which is then not enough to completely cover the electrode surface. This is further supported by similarities between spectra at bare glassy carbon electrodes (not shown) and polymer-modified electrodes after polymerisation with the 1.6 V limit.

The values of R_Ω were almost the same for each film (1.7 $\pm$ 0.3 Ω cm^2), which therefore seems to be dominated by the resistance of the electrolyte solution. The values of CPE_1 increased with increasing positive potential; this can be due to the increase in the electroactive area of the electrode which

Fig. 5 Complex plane impedance spectra of **a** poly(4A3HN1SA)/GCE in 0.5 M H$_2$SO$_4$ after polymerisation between −0.8 V and 1.6, 1.8 and 2.0 V; (**b–d**) poly(4A3HN1SA)/GCE, poly(4AN1SA)/GCE and poly(7A4HN2SA)/GCE in B-R buffer solutions of **b** pH 4 and **c, d** pH 7. Spectra (**a–c**) recorded at potentials close to the midpoint between the potentials of the major anodic and cathodic peaks in the cyclic voltammograms of the polymers in each medium and **d** outside the redox peak region. *Lines* show equivalent circuit fitting to the circuits in Fig. 6. See text for further details

Fig. 6 Equivalent electrical circuits used to fit the experimental impedance spectra in Fig. 5. R_Ω is the cell resistance, R_{ct} the charge transfer resistance, CPE a constant phase element and Z_W a Warburg impedance

allows faster charge and discharge of the interfacial double layer [31]. The α_1 value for CPE$_1$ is also the lowest for the 1.6 V positive limit, which could be due to the partial coverage of the glassy carbon electrode and thence greater surface non-uniformity.
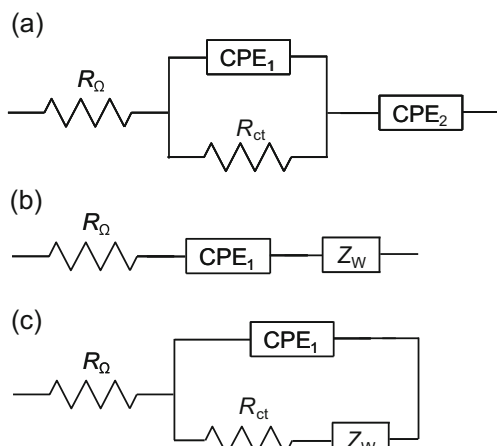
In relation to the linear diffusion, the linear diffusion resistance is only a little larger for the polymer film formed at +2.0 V than at 1.8 V (see Table 1), but the time constant is double that mainly reflects the fact that the polymer film is thicker (evidence from higher peak currents in cyclic voltammetry).

Electrochemical impedance spectra using the three different polymer-modified electrodes were then recorded in B-R buffer solutions of pH 4.0 and 7.0, Fig. 5b–d. Results from fitting the spectra are summarised in Table 4.

In pH 4.0 solution, Fig. 5b, spectra were recorded at the potentials −0.11, 0.04 and 0.12 V (vs. Ag/AgCl) using poly(4A3HN1SA)/GCE, poly(4AN1SA)/GCE and poly(7A4HN2SA)/GCE, respectively. The values of applied potential were chosen to be close to the midpoint between the anodic and cathodic peak potentials of the polymers' respective major peaks at the specified pH. All the spectra were fitted by the same equivalent circuit of Fig. 6b consisting of R_Ω in series with CPE$_1$ and Z_W. A higher CPE value is observed at poly(4A3HN1SA)/GCE, while poly(4AN1SA)/GCE and poly(7A4HN2SA)/GCE have almost the same values. The Warburg diffusion resistance obtained using poly(7A4HN2SA)/GCE is about half of that obtained using

Table 3 Equivalent circuit element values obtained by fitting of the impedance spectra after 4A3HN2SA polymerisation between −0.8 V and different positive potential limits

Positive limit/V	$R_\Omega/\Omega\ cm^2$	$R_{ct}/\Omega\ cm^2$	$CPE_1/mFcm^{-2}\ s^{\alpha-1}$	α_1	$CPE_2/mFcm^{-2}\ s^{\alpha-1}$	α_2	$R_W/\Omega\ cm^2\ s^{\alpha-1}$	τ/s	α
1.6	1.98	13.8	6.17	0.58	0.68	0.86	–	–	–
1.8	1.68	–	13.7	0.80	–	–	1.59	0.004	0.47
2.0	1.51	–	17.5	0.70	–	–	1.89	0.008	0.48

poly(4A3HN1SA)/GCE and poly(4AN1SA)/GCE. This is an indication of the porosity (see SEM below) and easier diffusion of species through the poly(7A4HN2SA) film.

At pH 7.0, Fig. 5c, spectra were recorded at potentials −0.20, −0.09 and −0.05 V (vs. Ag/AgCl) using poly(4A3HN1SA)/GCE, poly(4AN1SA)/GCE and poly(7A4HN2SA)/GCE, respectively. The equivalent circuit used to fit the spectra of poly(4AN1SA)/GCE and poly(7A4HN2SA)/GCE is the same as the circuit used at pH 4.0 (Fig. 6b). However, the spectrum of poly(4A3HN1SA)/GCE at low frequency shows the beginning of a semicircle, Fig. 5c, and was fitted better with a Randles-type circuit (Fig. 6c). This difference shows the greater effect of pH change on poly(4A3HN1SA)/GCE compared to the other two modified electrodes.

There is intense interest in materials that can perform well around physiological pH at different potentials, such as in biosensors. Therefore, spectra of the polymers in pH 7.0 solution were also investigated outside their redox region. Spectra were recorded at potentials −0.50 V for poly(4A3HN1SA)/GCE and −0.25 V for both poly(4AN1SA)/GCE and poly(7A4HN2SA)/GCE. At these negative applied potentials, a semicircle corresponding to a high charge-transfer resistance together with Warburg diffusion is observed (Fig. 5d). All spectra were fitted well by a Randles-type circuit (Fig. 6c). From the circuit fitting values, R_{ct} is dominant, an indication of a mainly charge transfer controlled process, most probably due to traces of oxygen in the solution. The values of charge-transfer resistance increased in the order poly(7A4HN2SA)/GCE, poly(4AN1SA)/GCE and poly(4A3HN1SA)/GCE, indicating a faster electron transfer process at poly(7A4HN2SA)/GCE.

The values from the fittings of experimental results are almost the same for poly(7A4HN2SA)/GCE in pH 4.0 and 7.0 solutions while significant changes are observed at poly(4A3HN1SA)/GCE and poly(4AN1SA)/GCE. This is in agreement with cyclic voltammetry in solutions of different pH, showing the stability and better electrochemical activity of poly(7A4HN2SA) films over a broad pH range. In the case of poly(4AN1SA)/GCE, the change in solution pH from 4.0 to 7.0 led to a decrease in both the Warburg diffusion resistance and the CPE values by a factor of two. The value of R_Ω also decreased for all polymer film modified electrodes with increasing pH, which cannot be ascribed to the change in the composition of the supporting electrolyte with the addition of Na^+ and OH^- ions with removal of protons, and suggests some small irreversible polymer film degradation.

Comparison of the CPE α values in both pH 4.0 and 7.0 solution inside and outside the redox region, the smallest is obtained using poly(7A4HN2SA)/GCE and higher and comparable values are observed for both poly(4A3HN1SA)/GCE and poly(4AN1SA)/GCE. This reflects the greater porosity

Table 4 Equivalent circuit element values obtained by fitting the impedance spectra of poly(4A3HN1SA)/GCE, poly(4AN1SA)/GCE and poly(7A4HN2SA)/GCE recorded in B-R buffer solution of pH 4.0 and 7.0

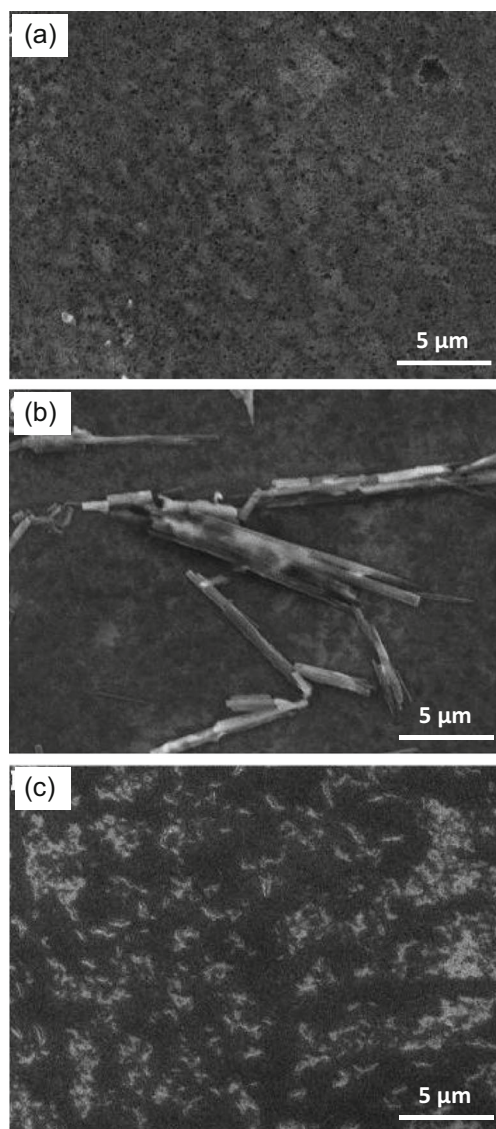| pH	Electrode	E_{ap}/V	$R_\Omega/\Omega\ cm^2$	$R_{ct}/k\Omega\ cm^2$	$CPE_1/mF\ cm^{-2}s^{\alpha-1}$	α_1	$R_W/\Omega\ cm^2\ s^{\alpha-1}$	τ/s	α
4.0	poly(4A3HN1SA)/GCE	−0.11	40	–	2.25	0.92	9.38	0.003	0.21
	poly(4AN1SA)/GCE	0.04	40	–	1.68	0.91	8.99	0.003	0.25
	poly(7A4HN2SA)/GCE	0.12	43	–	1.69	0.83	4.20	0.003	0.22
7.0	poly(4A3HN1SA)/GCE	−0.20	24	3.11	1.18	0.91	7.46	0.003	0.26
	poly(4AN1SA)/GCE	−0.09	25	–	0.90	0.89	3.67	0.003	0.24
	poly(7A4HN2SA)/GCE	−0.05	21	–	1.77	0.86	4.61	0.003	0.29
7.0	poly(4A3HN1SA)/GCE	−0.50	26	6.83	0.51	0.91	2.25	0.003	0.19
	poly(4AN1SA)/GCE	−0.25	25	4.65	0.74	0.91	4.93	0.003	0.25
	poly(7A4HN2SA)/GCE	−0.25	21	3.39	0.87	0.82	3.53	0.003	0.20

Fig. 7 Scanning electron microscopy images of films on ITO electrodes prepared in 0.1 M HNO₃ solution containing 2 mM **a** 4A3HN1SA, **b** 4AN1SA and **c** 7A4HN2SA

microstructures. The microstructures are composed of uniformly distributed fibres, particles and small pores.

The surface of poly(4AN1SA), Fig. 7b, consisted of well-defined tubular structures randomly distributed on top of a sponge-like homogenous surface. The tubes are about 1 μm in diameter and stretch up to 30 μm in length. Such tubular structures are known in polymers and co-polymers of aniline with different naphthalene sulfonic acids as doping agents or co-monomers. The formation yield, tubular morphology, size and electrical properties of the nanostructures obtained were reported to depend on the position and number of –SO₃H groups attached to the naphthalene ring as well as the synthesis conditions [22, 32]. Moreover, the possibility of synthesising such nanotubes of conducting polymers is very important for the applications in controlled drug delivery and neural interfaces [2].

The presence of the relatively homogeneous spongy-like surface below the tubes of poly(4AN1SA) seems to be a background film on which the tubular structures grow. This might be due to the change in the mechanism of polymer deposition when the film becomes thick, and a direct access of unreacted monomers to the electrode surface is inhibited [25]. The texture of the underlying film also resembles the polymer film poly(4A3HN1SA), in agreement with EIS results showing comparable surface homogeneity and smoothness.

The image of poly(7A4HN2SA), Fig. 7c, showed isolated-, spherical- and irregular-shaped growths of different sizes unevenly distributed over the surface. The dispersed distributed isolated structures accounted for the lack of smoothness and homogeneity of poly(7A4HN2SA)/GCE, as deduced from the analysis of the impedance spectra.

Conclusions

The electrosynthesis, characterisation and comparison of new conducting polymers from 4-amino-3-hydroxynaphthalene-1-sulfonic acid (4A3HN1SA), 4-aminonaphthalene-1-sulfonic acid (4AN1SA) and 7-amino-4-hydroxynaphthalene-2-sulfonic acid (7A4HN2SA) are reported. The electropolymerisation of 4AN1SA and 7A4HN2SA and characterisation of the polymer-modified electrodes is reported for the first time.

Polymerisation parameters were optimised using 4A3HN1SA and results showed the need to apply a sufficiently high positive potential limit to allow better film formation. The three polymers were synthesised under similar electropolymerisation conditions. Characterisation of the polymer films was done using cyclic voltammetry, electrochemical impedance spectroscopy and scanning electron microscopy. Despite the presence of similar functional groups in

and non-homogeneity of the poly(7A4HN2SA) film compared to poly(4A3HN1SA) and poly(4AN1SA), which form films of better and comparable homogeneity and smoothness.

Morphology

Figure 7 shows scanning electron microscopy (SEM) images of the polymer films of 4A3HN1SA, 4AN1SA and 7A4HN2SA on ITO. The micrographs show clear differences in the morphologies of the three substituted naphthalene sulfonic acid-based polymer films that can be attributed to the difference in reactivities of the monomers and polymer growth during film formation.

The poly(4A3HN1SA) film on ITO, Fig. 7a, exhibited a homogeneously and densely distributed irregular

the monomers, the resulting polymers showed distinct properties and behaviour, which could be due to the difference in the reactivities of the monomers and reaction routes for film formation, which in turn led to different relative positions of functional groups in the polymer backbone. SEM showed that poly(7A4HN2SA), which demonstrated the best stability in solutions of higher pH up to 9, formed a porous and non-uniform film, whereas poly(4A3HN1SA) has a homogeneous irregular microstructure; tubular and microstructures were observed in the micrographs of poly(4AH1SA) films.

These results show the potential utility of these substituted naphthalene sulfonic acid polymers in various applications, such as chemical sensors, neural interfaces, anti-corrosive materials, energy storages, drug delivery and electroluminescence devices, especially when applications require stable films over a broad pH window.

References

1. Inzelt G (2012) Conducting polymers. A new area in electrochemistry, 2nd edn. Springer, Heidelberg, Germany
2. Asplund M, Nyberg T, Inganäs O (2010) Electroactive polymers for neural interfaces. Polym Chem 1:1374–1391
3. Zhu G, Zu J, Yue R, Lu B, Hou J (2012) Novel poly-bridged-naphthalene with blue-light-emitting property via electropolymerization. J Appl Polym Sci 123:2706–2714
4. Murphy LJ (1998) Reduction of interference response at a hydrogen peroxide detecting electrode using electropolymerized films of substituted naphthalenes. Anal Chem 70:2928–2935
5. Pham MC, Bouallala S, Le LA, Dang VM, Lacaze PC (1997) Study of a heteropolyanion-doped poly(5-amino-1-naphthol) film electrode and its catalytic activity. Electrochim Acta 42:439–447
6. Balamurugan A, Chen SM (2007) Poly(3,4-ethylenedioxythiophene-co-(5-amino-2-naphthalenesulfonic acid)) (PEDOT-PANS) film modified glassy carbon electrode for selective detection of dopamine in the presence of ascorbic acid and uric acid. Anal Chim Acta 596: 92–98
7. D'Eramo F, Marioli JM, Arevalo AA, Sereno LE (1999) HPLC analysis of carbohydrates with electrochemical detection at a poly-1-naphthylamine/copper modified electrode. Electroanalysis 11:481–486
8. Geto A, Tessema M, Admassie S (2014) Determination of histamine in fish muscle at multi-walled carbon nanotubes coated conducting polymer modified glassy carbon electrode. Synth Met 191:135–140
9. Geto A, Amare M, Tessema M, Admassie S (2012) Polymer-modified glassy carbon electrode for the electrochemical detection of quinine in human urine and pharmaceutical formulations. Anal Bioanal Chem 404:525–530
10. Geto A, Amare M, Tessema M, Admassie S (2012) Voltammetric determination of nicotine at poly(4-amino-3-hydroxynaphthalene sulfonic acid)-modified glassy carbon electrode. Electroanalysis 24:659–665
11. Won MS, Yoon JH, Shim YB (2005) Determination of selenium with a poly(1,8-diamino-naphthalene)-modified electrode. Electroanalysis 17:1952–1958
12. Zewde BW, Admassie S (2012) Electrocatalysis of oxygen reduction at poly(4-amino-3-hydroxynaphthalene sulfonic acid) and platinum loaded polymer modified glassy carbon electrodes. J Power Sources 216:502–507
13. Tasch S, Graupner W, Leising G, Pu L, Wagner MW, Gruhbs RH (1995) Red-orange electroluminescence with new soluble and air-stable poly(naphthalene-vinylene)s. Adv Mater 7:903–906
14. Huang Z, Shi L, Qu L, Hong X (2003) Electrochemical polymerization of β-naphthalene sulfonic acid in the mixed electrolyte of boron trifluoride diethyl etherate and trifluoroacetic acid. J Electroanal Chem 544:41–46
15. Mori T, Kijima M (2009) Synthesis and electroluminescence properties of carbazole-containing 2,6-naphthalene-based conjugated polymers. Eur Polym J 45:1149–1157
16. Mori T, Kijima M (2007) Synthesis and optical properties of polynaphthalene derivatives. Opt Mater 30:545–552
17. Bhandari H, Choudhary V, Dhawan SK (2011) Influence of self-doped poly(aniline-co-4-amino-3-hydroxy-naphthalene-1-sulfonic acid) on corrosion inhibition behaviour of iron in acidic medium. Synth Met 161:753–762
18. Meneguzzi A, Ferreira CA, Pham MC, Delamar M, Lacaze PC (1999) Electrochemical synthesis and characterization of poly(5-amino-1-naphthol) on mild steel electrodes for corrosion protection. Electrochim Acta 44:2149–2156
19. Meneguzzi A, Pham MC, Lacroix JC, Piro B, Adenier A, Ferreira CA, Lacaze PC (2001) Electroactive poly(aromatic amine) films for iron protection in sulfate medium. J Electrochem Soc 148:B121–B126
20. Yildiz R, Dogan T, Dehri I (2014) Evaluation of corrosion inhibition of mild steel in 0.1 M HCl by 4-amino-3-hydroxynaphthalene-1-sulphonic acid. Corros Sci 85:215–221
21. Bereket G, Hur E (2009) The corrosion protection of mild steel by single layered polypyrrole and multilayered polypyrrole/poly(5-amino-1-naphthol) coatings. Prog Org Coat 65:116–124
22. Bhandari H, Bansal V, Choudhary V, Dhawan SK (2009) Influence of reaction conditions on the formation of nanotubes/nanoparticles of polyaniline in the presence of 1-amino-2-naphthol-4-sulfonic acid and applications as electrostatic charge dissipation material. Polym Int 58:489–502
23. Ramachandran R, Kathiravan R, Rani M, Kabilan S, Jeong YT (2012) Synthesis and characterization of novel conducting 1,5-naphthalenediamine–aniline copolymer. Synth Met 162:1636–1642
24. Marjanovic GC, Trchova M, Matejka P, Holler P, Marjanovic B, Juranic I (2006) Electrochemical oxidative polymerization of sodium 4-amino-3-hydroxynaphthalene-1-sulfonate and structural characterization of polymeric products. React Funct Polym 66:1670–1683
25. Thiemann C, Brett CMA (2001) Electrosynthesis and properties of conducting polymers derived from aminobenzoic acids and from aminobenzoic acids and aniline. Synth Met 123:1–9
26. Vorotyntsev MA, Zinovyeva VA, Konev DV (2010) In: Cosnier S, Karyakin A (eds) Electropolymerization: concepts, materials and applications. Wiley-VCH Verlag GmbH & Co. KGaA, Weinheim, Germany

27. Kumar SA, Chen SM (2007) Electrochemically polymerized composites of conducting poly(*p*-ABSA) and flavins (FAD, FMN, RF) films and their use as electrochemical sensors: a new potent electroanalysis of NADH and NAD$^+$. Sensor Actuat B 123:964–977

28. Enache T, Oliveira-Brett AM (2015) Phenol and para-substituted phenols electrochemical oxidation pathways. J Electroanal Chem 655:9–16

29. Laviron E, Roullier L, Degrand C (1980) A multilayer model for the study of space distributed redox modified electrodes. Part II: theory and application of linear potential sweep voltammetry for a simple reaction. J Electroanal Chem 112:11–23

30. Wei Z, Wan M (2003) Synthesis and characterization of self-doped poly(aniline co-aminonaphthalene sulfonic acid) nanotubes. J Appl Polym Sci 87:1297–1301

31. Barsan MM, Pinto EM, Florescu M, Brett CMA (2009) Development and characterization of a new conducting carbon composite electrode. Anal Chim Acta 635:71–78

32. Zhang Z, Wei Z, Zhang L, Wan M (2005) Polyaniline nanotubes and their dendrites doped with different naphthalene sulfonic acids. Acta Mater 53:1373–1379